

THERMOKINETIC PROCESSES IN THE CORIUM TRAPS OF HIGH-TEMPERATURE MELT DURING THE REACTOR ACCIDENTS AT AN A-PLANT: SIMULATION

A.N. Kovalenko^{1,3}, A.O. Koptyukhov², D.K. Meshcheryakov³, A.P. Schuklinov^{3,4}

¹ Ioffe Physical Technical Institute of the Russian Academy of Sciences, St. Petersburg, Russian Federation;

² NRC "Kurchatov Institute" – PNPI, Gatchina of Leningrad region, Russian Federation;

³ Peter the Great St. Petersburg Polytechnic University, St. Petersburg, Russian Federation;

⁴ JSC "Atomproekt", St. Petersburg, Russian Federation

The two-stage model of changing the thermal and phase state of the active zone melt in the cooled subreactor crucible trap when interacting with the sacrificial material and when crystallizing the diluted corium after the gravitational inversion of its oxide and metal components is presented. The simulation is based on the generalized formulation of Stefan's task. The results of the end-to-end calculation of the COMSOL Multiphysics package show that the thermokinetic processes examined generally reduce the temperature and density of the corium, reduce heat flows on the trap body, minimize the release of hydrogen and radioactive fission products with their retention in a controlled thermal and phase state until full crystallization.

Keywords: melt active zone, subreactor crucible trap, sacrificial material, thermal state

Citation: Kovalenko A.N., Koptyukhov A.O., Meshcheryakov D.K., Schuklinov A.P., Thermokinetic processes in the corium traps of high-temperature melt during the reactor accidents at an a-plant: simulation, St. Petersburg Polytechnical State University Journal. Physics and Mathematics. 13 (4) (2020) 46–58. DOI: 10.18721/JPM.13405

This is an open access article under the CC BY-NC 4.0 license (<https://creativecommons.org/licenses/by-nc/4.0/>)

Introduction

Data on severe accidents at nuclear power plants indicate that the physical causes are related to critical disruption of heat removal from the reactor core, with reactor elements overheating and melting as a result [1–3]. Technical solutions for retaining the corium melt (a mixture of uranium, plutonium, zirconium oxides, fragments of nuclear fuel fission, absorbing materials, metals of support structures such as iron, nickel, chromium, etc.) in the reactor, developed for external vessel cooling in reactors with low and medium power [4], proved to be unreliable for preventing wall melting in high power reactor vessels. As an alternative [5], the concept of ex-vessel melt retention devices (MRD) was proposed for this type of reactors as an additional barrier for the propagating reaction products, confining them in a controlled thermal and phase state until complete crystallization.

For European EPR reactors, this concept is implemented based on a lateral compartment for melt spreading, cooled from above by water [6]. Subreactor crucible traps with filler made of sacrificial material (SM), cooled by water from the outside, are used as heat exchangers in Russian VVER reactors [7] (Fig. 1).

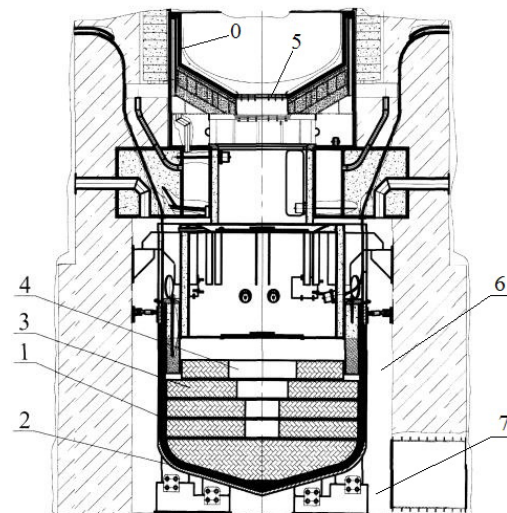


Fig. 1. Schematic of crucible-type melt retention devices for Russian NPPs with VVER reactors reactor vessel 0; cooled trap 1; MRD supports 2; pellets 3 of sacrificial material (SM); assembly 4 of the container holding the SM; melt plug 5; lateral heat exchanger 6; channel supplying cooling water and lower heat exchanger 7 (according to RF patent 2514419 [7])



Combining the functions of a water-cooled crucible for trapping the melt and a collector with the SM in the MRD greatly expands the range of problems considered, especially since the composition of the incoming melt may be unclear and there is insufficient data on its interaction with the sacrificial material [8–10].

Full-scale studies of these processes are impossible; moreover, small-scale setups only offer limited possibilities to reproduce them. For this reason, mathematical modeling is very important for understanding the physical mechanisms underlying the retention of the corium melt captured by the trap in controlled thermal and phase states, as well as for substantiating the technical solutions adopted.

Notably, solving these problems via well-known specialized software codes developed for modeling various scenarios of severe accidents and their individual stages at the in-reactor stage may be considerably difficult for a number of reasons. Practical experience accumulated in computational studies of crucible traps [11–15] with some of these codes (SOCRAT, GEFEST-ULR, KORSAR, ASTEC), as well as benchmarking of these and other codes at the Joint Research Center (JRC) of the Directorate for Energy, Transport and Climate of the European Commission (Petten, Netherlands) [16] indicates that there is a large scatter of data both between different codes and between different users of the same code. This can be largely due to the differences not only in approaches to constructing physical and mathematical models but also in nodalization schemes, computational algorithms and criteria for evaluating the results obtained.

In this regard, the approach accounting for the interrelated factors characterizing thermokinetics and chemical phase, with the possibility of end-to-end computations of conjugated mechanical, thermal, hydrodynamic and chemical phenomena has certain benefits for simulating the processes of interaction of the sacrificial material with the melt in a crucible trap and subsequent changes in its state up to complete crystallization.

Thermokinetic processes in the crucible trap

The processes of interaction between the high-temperature corium melt and the energy-absorbing components of the sacrificial material melting in the corium, consisting of a mixture of light iron oxides Fe_2O_3 and aluminum Al_2O_3 , occur in a water-cooled crucible trap. The above processes must meet certain requirements:

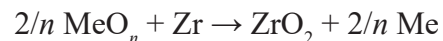
provide a reduction in corium temperature and density, as well as a reduction in heat fluxes to the trap body;

preserve the subcriticality of the melt;

minimize the yields of hydrogen and radioactive fission products [9, 10, 17, 18].

The relationships between mass and heat transfer, substance transformations and conversion of various types of energy in these processes are determined by a set of coupled physical phenomena of mechanics, thermal physics, hydrodynamics, and nuclear physics.

A significant role in these relationships is played by chemical reactions of endothermic reduction of oxides from the composition of the sacrificial material and exothermic oxidation of unoxidized elements of the melt, including zirconium by the redox reaction



(Me is the metal, n is its oxidation degree), helping to minimize hydrogen release during vapor-zirconium contact.

The thermal effects of these reactions are comparable in power to the magnitude of residual heat release of fission products and their nuclear transformations [9, 10, 19]. It is of great practical interest to explore the mechanism of interaction between the sacrificial oxide material and the melt containing strong reducing agents in the liquid-phase combustion mode with a total endothermic effect in the reaction zone [20]. It can occur if the products of chemical interaction are in liquid or dispersed in liquid state with both metalized and oxidized component of the melt.

Additional dilution of corium due to the unreacted part of the melted iron and aluminum oxides from the composition of SM leads to a noticeable decrease in the density of the oxide components of the melt initially appearing, heavier compared to the metal ones, and the subsequent gravitational inversion of their initial stratification. This makes it possible to additionally supply cooling water to the melt surface without the risk of steam explosion [21].

In this case, a refractory skull crust forms under non-isothermal conditions, preventing mass and heat transfer both on the surface of the corium and between its immiscible oxide and metal layers. There is also a risk that crystallization zones of individual melt components may form, with secondary centers of increased radioactivity appearing where heavier (relative to the entire melt) oxides of radioactive matter locally accumulate. To

preserve subcriticality, the composition of SM includes immobilizing radionuclide additives of refractory heavy elements, such as gadolinium oxide, which absorb thermal neutrons [18]. Localization of heavy oxides with large residual heat generation can also lead to boiling of uranium dioxide with release of components into the gas phase, with an ablative interaction with the steel wall of the trap body itself, melting with insufficient external cooling [8].

Correct analysis of the processes occurring in the interaction of corium and sacrificial materials is associated with taking into account the phase transformations of the components when changing the composition and thermodynamic parameters of the system, reflected in experimental or calculated phase state diagrams.

Experimentally obtaining the full diagram for this system is very resource-intensive and the proportions of the corium composition are uncertain, due to the large number of parameters of the possible mechanism for its formation in the nodalization scheme adopted (according to the estimates conducted in [22], the number of parameters is about 10^3-10^4), so this stage replaced by construction of computed diagrams characterizing the composition, conditions, and properties based on the chemical thermodynamics of phases of variable composition [9].

Problem statement

We consider the phase equilibrium approximation of multicomponent thermodynamic systems with variable composition for a two-stage mathematical model of thermokinetic processes in the corium melt trap, describing the set of thermal, chemical and hydrodynamic phenomena occurring, as well as correlated thermodynamic factors, taking into account the results of laboratory studies at small-scale facilities [23].

At the first, 'pre-inversion' stage, the mathematical model is formulated as a Stefan problem for a material environment of the corium trap with mobile heat sources of endothermic decomposition of the melting SM, heat of exothermic reactions of chemical interaction with the SM of underoxidized zirconium, chromium, and uranium entering into the trap in the core melt, and also the heat of residual heat release of radioactive elements. In this case, the isotherm corresponding to the melting temperature of the SM components divides the computational domain into subregions, where the condition of continuity

for temperature and the condition for changing the heat flux density by a value equal to the product of the enthalpy of phase transition by the normal component of the velocity of the interface are imposed at the boundary. In a generalized form [24], this problem is reduced to a single nonlinear heat conduction and mass transfer equation in the entire melt region, which includes the above nonuniform conjugation conditions for temperature and heat flux at the previously unknown (free) interfaces directly into the equation itself:

$$c_{eff} \rho \left(\frac{\partial T}{\partial \tau} + \mathbf{v} \text{grad } T \right) = \text{div}(\lambda \text{grad } T) + f. \quad (1)$$

Here ρ , kg/m^3 , is the density of the medium component; T , K , is the temperature; τ , s , is the time; \mathbf{v} , m/s , is the local velocity of the medium (vector); λ , $\text{W/(m}\cdot\text{K)}$, is the heat transfer coefficient; the term $(\mathbf{v} \text{grad } T)$ accounts for the temperature change due to convective transport of the medium; f , W , defines the power of internal heat sources; c_{eff} , $\text{J/(kg}\cdot\text{K)}$, defines the effective specific heat capacity, accounting for the heat of the phase transition at its boundary in concentrated form.

During melting, the derivative function for the effective heat capacity is as follows:

$$c_{eff} = c_{p,sol} \cdot (1 - \varphi(T)) + c_{p,liq} \cdot \varphi(T) + \delta(T - T_{mel}) L \frac{d\varphi}{dT}, \quad (2)$$

where $c_{p,sol}$, $c_{p,liq}$, $\text{J/(kg}\cdot\text{K)}$, are the heat capacities of the solid and liquid phases, respectively; $\varphi(T)$ is the phase transition fraction function determined by the equilibrium phase diagram of the system; L , J/kg , is the specific heat capacity of the phase transition; $\delta(T)$ is the delta function; T_{mel} , K , is the phase transition temperature.

The model takes into account heat fluxes not only in the reaction layer at the mobile boundaries of phase transitions but also in the volume of interacting materials, including those caused by residual heat release from products of nuclear transformations and heat exchange of the corium melt with the SM. The intensity of the heat exchange depends both on the kinetics of the ongoing chemical reactions, which depends in turn on the temperature conditions of activation (primarily, the initial temperature of the incoming melt), and on the mixing rate of the reaction products with the corium melt, which is assumed to be instantaneous.

The heat transfer during natural convection in the melt is based on unsteady Reynolds-averaged Navier–Stokes equations for a viscous incompressible fluid, which determine the effect of convective velocity fluctuations in the form of turbulent kinetic energy of the fluctuations and its dissipation due to internal friction:

$$\begin{aligned} & \rho \frac{\partial \mathbf{v}}{\partial \tau} + \rho(\mathbf{v} \cdot \nabla) \mathbf{v} = \\ & = \nabla[-p\mathbf{I} + (\mu + \mu_m)(\nabla \mathbf{v} + (\nabla \mathbf{v})^T)] - \\ & - \frac{2}{3}(\mu + \mu_B)(\nabla \mathbf{v})\mathbf{I} - \frac{2}{3}\rho k\mathbf{I}] + \rho \mathbf{g}. \end{aligned} \quad (3)$$

Here ρ , kg/m³, is the bulk density; \mathbf{v} , m/s, is the flow velocity (vector); p , Pa, is the pressure; μ , Pa·s, is the dynamic viscosity; μ_m , Pa·s, is the turbulent viscosity; \mathbf{g} , m²/s, is the free fall acceleration (vector); k , J, is the turbulent kinetic energy (turbulent fluctuations, $k = \sum_i (\overline{V_i'^2}/2)$); the subscript T denotes the transposed tensor; ∇ is the Hamiltonian operator; \mathbf{I} is the unit tensor.

The equation for turbulent kinetic energy k and its dissipation rate ε , due to viscous friction

$$\mu_m = \rho c_\mu k^2/\varepsilon,$$

is closed in accordance with the standard (k - ε) turbulence model [25].

In the given conditions, when the intensity of turbulent heat transfer is caused by the thermogravitational mechanism of turbulent energy generation, its value depends on the established regime of thermal stratification of oxide and metal layers of the corium. The stability of thermal stratification depends on the direction of heat supply and removal through the boundaries of the layer relative to the vector of gravity.

Eq. (3) is solved together with the continuity equation:

$$\nabla \cdot (\rho \mathbf{v}) = 0. \quad (4)$$

For hydrodynamic equations, the usual no-slip conditions are imposed at the contact interface with the body, and the sliding condition along the symmetry axis and the upper free boundary (the normal velocity components are equal to zero). In the case of crust formation, the no-slip condition is also imposed at the upper boundary.

For the temperature problem on the side and bottom faces of the melt pool, contacting the cooled walls of the trap body, third-kind boundary conditions of heat transfer are imposed at a given temperature T_{cool} of the cooling water

and the heat transfer coefficient α :

$$q_{cool} = -\lambda(\partial T / \partial h) = \alpha(T - T_{cool}), \quad (5)$$

where h is the normal to the surface, the heat transfer coefficient α was computed for well-developed steady flow in the annular channel of the water cooling jacket of the outer walls of the trap body according to recommendations in [26].

The initial thermal state of the filled trap corresponds to the temperature of the oxide and metal components of the melt of 3000 K and the temperature of the sacrificial material of 400 K.

In the second, ‘post-inversion’ stage of the melt pool at $L = 0$ and $\varphi(T) = 1$, the cooling processes of the melt components after the gravitational inversion of its oxide and metal components are simulated, taking into account natural convection, external cooling of the trap body, and radiative heat transfer over the pool surface. The oxide and metal components of the inverted melt layers are assumed to be homogeneous in structure. The given third-kind boundary conditions are preserved for heat transfer on the side and bottom surfaces of the melt pool contacting with the cooled walls of the trap body.

The conditions on the free surface of the pool, bordering the emitted aerosols, are complemented by accounting for heat transfer by radiation

$$\begin{aligned} & \lambda(\partial T / \partial h) + \alpha(T - T_{cool}) + \\ & + \varepsilon \sigma (T^4 - T_{mean}^4) = 0, \end{aligned} \quad (6)$$

where ε is the radiation coefficient (emissivity) of the melt surface, σ , W·m⁻²·K⁻⁴, is the Stefan–Boltzmann constant, T_{med} , K, is the temperature of the medium above the corium mirror.

The heat transfer coefficient α was taken into account based on the data from [21], when cooling water was supplied to the surface of the oxide melt using the dependence for film boiling of water on a solid upward-facing surface according to the recommendations in [26].

Initial conditions for this simulation stage are imposed according to the results of computations at the previous stage.

Decreasing the temperature of the melt components during cooling to their crystallization temperature at this model stage again leads to the Stefan problem. The differences between this statement and the one presented above are that the chemical heat of the interaction between the melt and the SM is not taken into account, while potential formation of spatial crystallization zones is accounted for, including those with a variable phase transition temperature, depending on

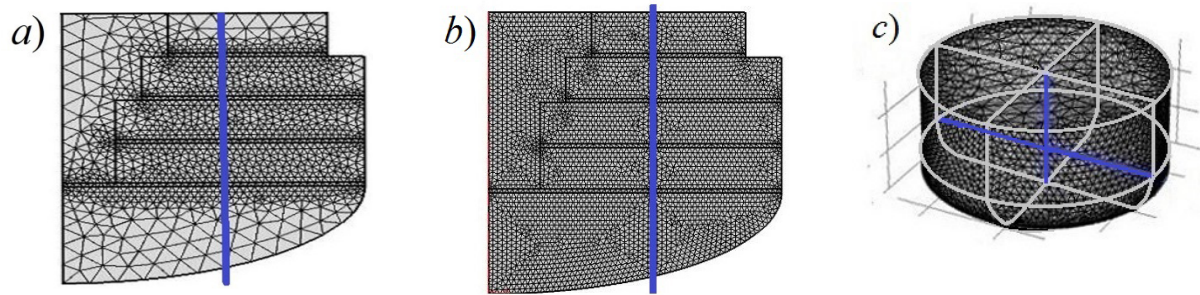


Fig. 2. Generated finite-element meshes for computed trap regions with selected control sections (blue lines) at different stages: at the ‘pre-inversion’ stage taking into account the initial location of the iron pellets (*a*) and their melting (*b*), and at the ‘post-inversion’ stage taking into account the location of the lighter oxide layer over the heavier metal layer, in the corium melt pool relative to the marked horizontal interface (*c*)

the location of solidus and liquidus lines in the phase diagram of the corium medium. Methods of thermodynamic analysis based on conditional minimization of Gibbs free energy using a set of different solution models are used to construct them [9].

Computational aspects

Simulation of the computational model was performed numerically using the COMSOL Multiphysics software package developed for modeling related multiphysics mechanical, thermal, electromagnetic, chemical, and hydrodynamic phenomena and systems [27]. This made it possible to carry out end-to-end computation of thermokinetic processes with phase transformations in the cooled high-temperature corium melt during its interaction with the sacrificial material both at the level of an individual structural element [28] and the SM container as a whole. Compatibility of the package with programming languages of Matlab/Simulink, AutoCAD, SolidWorks, Excel systems allows to include additional models for computing boundary conditions, setting material properties, etc.

The special modules available in the program automatically provide a suitable numerical discretization and solver configuration for a given mathematical model (1)–(6). In this case, the set is implemented based on the finite element method using the method of end-to-end counting with smoothing of coefficients without explicit separation of free interphase boundaries in the Stefan problem. After finding the solution, these boundaries were identified as isotherms corresponding to the temperatures of the considered phase transitions.

Initial geometric parameters of the trap, mass, composition and properties of various media and corium melt components, values of residual heat release power, characteristics of the sacrificial material and kinetics of chemical reactions were taken based on MRD designs for 1000–1200 MW VVER reactors.

The geometry of the problem solved was assumed to be two-dimensional axisymmetric. The generated meshes of the computational domain for the considered problems are shown at different simulation stages in Fig. 2.

The boundary layer was resolved using an anisotropic grid whose step decreased at the boundaries of the computational domain. The minimum size of the structural mesh element was 0.003 m and the maximum size was 0.119 m, for a total of 4,076,212 elements and the size of the computational domain of 2.74×2.85 m. The performed computations were compared with the results obtained at another minimum discretization step of 0.016 m, while the practical convergence of the solution remained at the same level.

Computational construction of the phase diagrams involved [9] for the components in the interaction system of the corium melt and sacrificial material was based on the TernAPI program for thermodynamic analysis, freely available from the website of Chemical Department of Moscow State University [29], using the algorithm of convex shells proposed.

Computational results and discussion

The results for computed changes in the thermal and phase states of the corium melt entering the trap during its interaction with the melting sacrificial material at the first, ‘pre-inversion’, stage of the simulation are shown in Figs. 3 and 4.

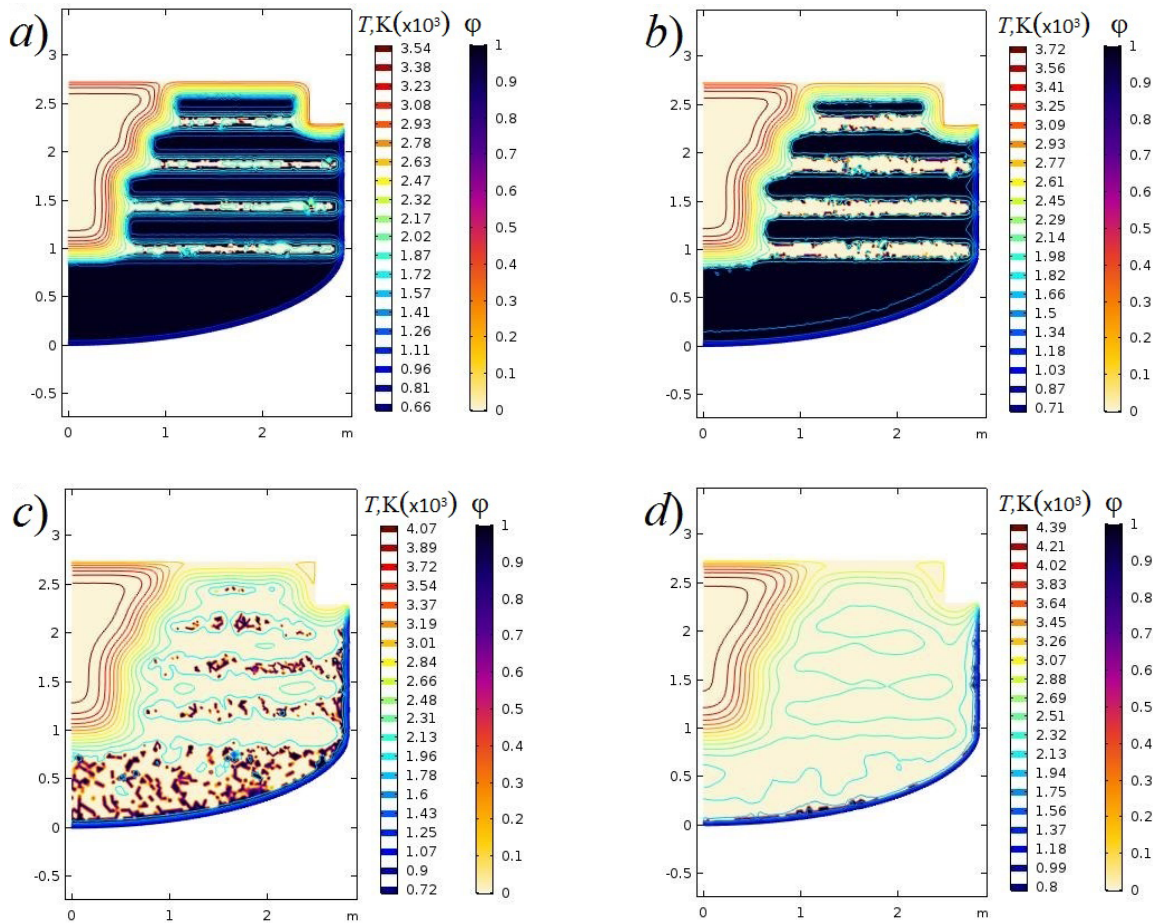


Fig. 3. Changes in temperature fields (T , K) and ratios ϕ of solid and liquid phases (dark and light regions, respectively) for corium and SM melt after it enters the trap and before inversion of oxide and metal components at different time points, min: in 10 (a) 30 (b), 60 (c), 90 (d). The ratio ϕ of solid to liquid phases is reflected by the color saturation in the range from 1 to 0

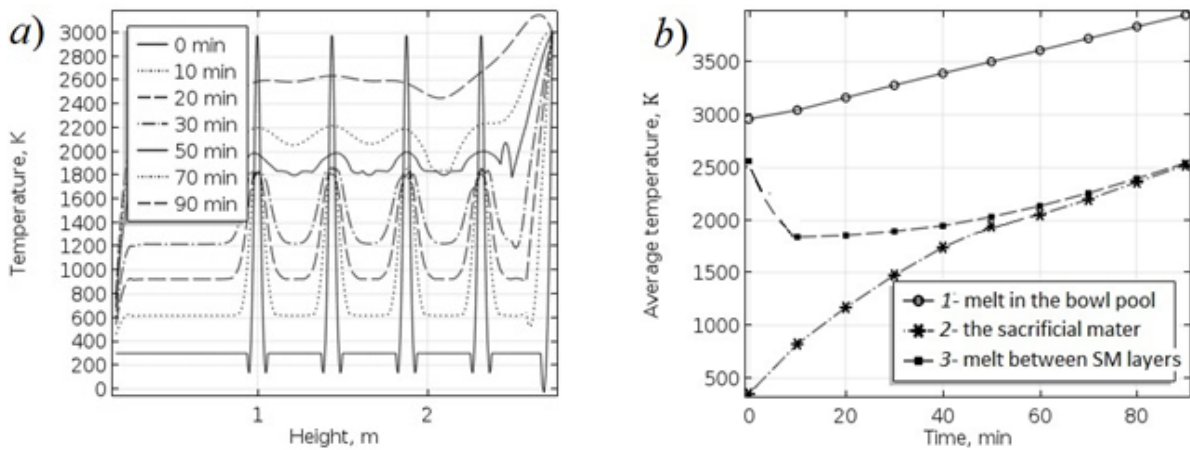


Fig. 4. Temperature distribution profiles in the control section of the trap (see Fig. 2, b) for different moments in time (a); mean temperatures over the corium (1) and SM (2) melt at the stages after entering the trap and before inversion of oxide and metal components (b). The stages shown are: melt inside the pool bowl 1, SM 2, melt between the pellet layers of SM 3

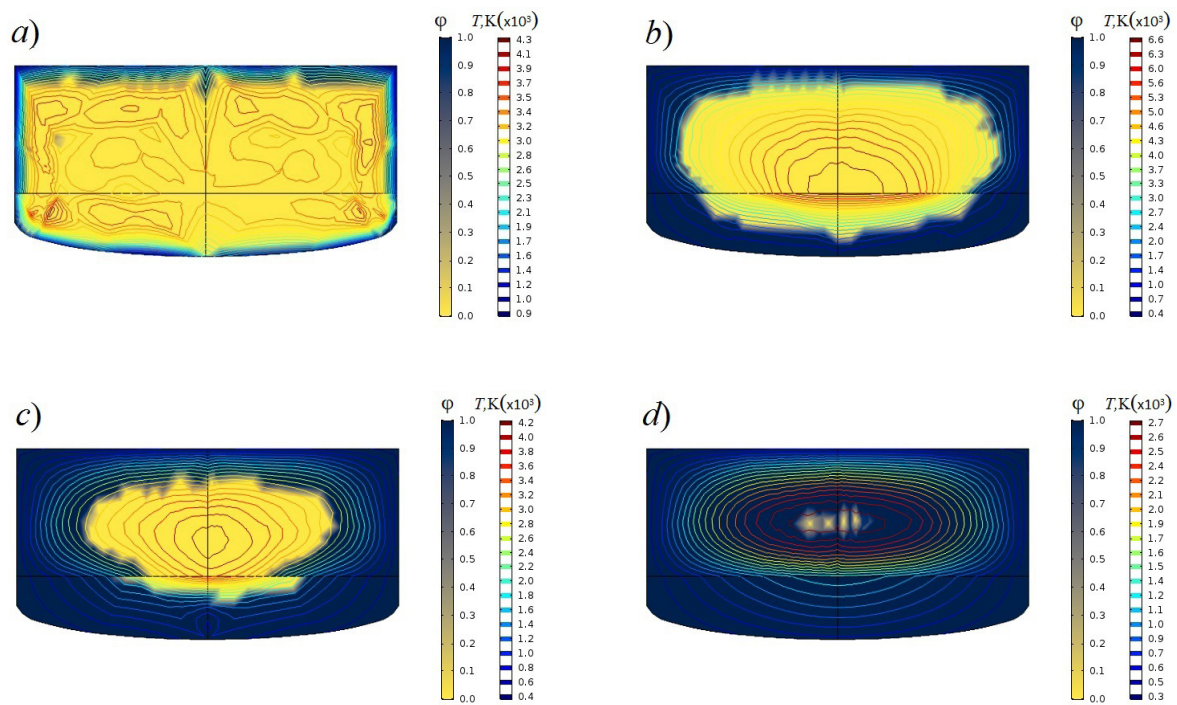


Fig. 5. Evolution of fields of temperature (T , K) and ratios φ for solid and liquid phases (dark and light regions, respectively) of the corium melt after its interaction with SM and inversion of oxide and metal components at different moments of time, h: after 5 (a) 40 (b), 65 (c), 78 (d)

Evidently, in the initial period, this interaction is accompanied by a decrease in the corium temperature, despite the residual heat release, due to the heat input for heating and melting of the sacrificial material. Thermokinetic processes are characterized by rather abrupt cooling of the high-temperature melt between the filler modules, up to its short-term solidification, which is replaced by overall melting together with the structural elements of the SM with redox reactions occurring between them.

Next, there is an increase in the temperature of the melt under the influence of residual energy release of radioactive elements. Together with additional dilution of the corium due to the unreacted part of the melted iron and aluminum oxides from the composition of the SM this leads to a noticeable decrease in the density of the oxide components of the melt initially arrived, heavier compared with the metal ones, and their rapid reverse gravitational inversion. Taking into account the estimated high rate of surfacing of the oxidized component and movement to the trap bottom of the metallized component [23], the duration of these processes is approximately 20–25 min at the stage of initial corium cooling and about

90–120 min before the final melting of the SM with inversion of the initial stratification of the metal and oxide layers of the melt.

Figs. 5 and 6 show computed results for the changes in thermal and phase states of the corium melt after chemical interaction with the SM and inversion of immiscible oxide and metal components of different densities, with molten oxides moving to the upper part and molten metals to the lower part of the melt pool.

The results of computations using the equations of motion for natural convection of the corium melt components are shown in Fig. 7.

Apparently, for the given directions of heat supply and removal through the boundaries of the upper oxide layer of the melt relative to the gravity vector, upward motion occurs in its central region and downward motion at the periphery near the cooled walls of the crucible. The motion of flows in the lower metal layer has an opposite character with unsteady thermal stratification under the interface with the oxide layer of the melt. According to the experimental data in [30], generation of turbulent flows of metal and oxide melts in free thermogravitational convection appears with the product of Grashof and Prandtl criteria

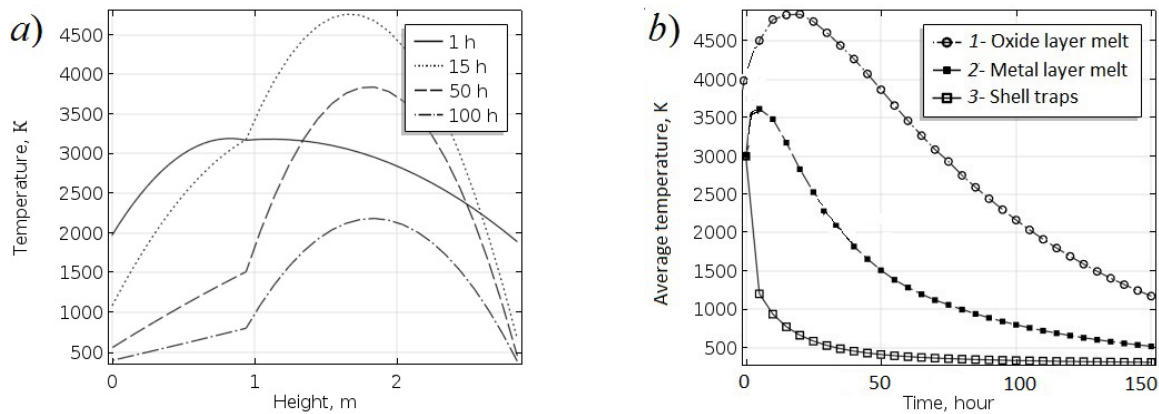


Fig. 6. Temperature distribution profiles in control section of the trap (see Fig. 2,c) for different moments of time (a) and average temperature values over the corium melt after inversion of oxide and metal components (b).

Data for oxide (1) and metal (2) melt layers, as well as for the trap shell (3) are shown

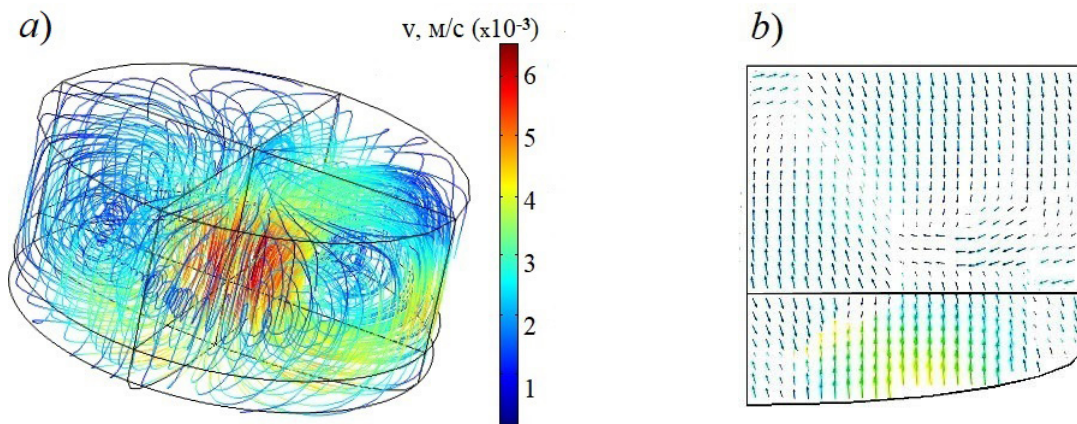


Fig. 7. Streamlines in the melt pool (a) and velocity field in its vertical section (b)

exceeding 47,000. For the parameters of the problem considered, this condition is satisfied with a large margin. Similar phenomena will be observed near the solidifying phase interface, since the melt is always superheated relative to the crystallization temperature.

After inversion of the melt components, the temperature of its oxide layer, where the sources of residual heat release are mainly concentrated, continues to grow for some time and, after reaching its maximum, begins to gradually decrease, as the trap body's side walls are cooled externally and water is supplied to the upper surface of the oxide layer of the melt, without risk of steam explosion [21].

The temperature of the metal layer changes almost synchronously due to heat transfer in its surface region adjacent to the oxide layer,

remaining below the temperature of the latter due to external cooling of the bottom of the trap body. Stabilization of thermal processes occurs after 10–20 h, with further transition to quasi-regular cooling of the melt. A slightly higher cooling rate of the metal layer and more fusible components cause its faster solidification, compared to the refractory components of the oxide layer. A fairly large molten core remains there for quite a long time (40–65 h), and even by 80 h separate pockets of the liquid phase remain in the crystallized zones. Throughout these processes, the heat fluxes from the corium to the trap walls are in the range from 0.2 to 0.6 MW/m², which does not exceed the critical heat load [14] on the external water-cooled surface of the crucible body with a sufficient margin.

Conclusion

The presented two-stage model of thermokinetic processes and the results of end-to-end computations of changes in thermal and phase states of the corium melt in the core entering the trap during severe accidents of NPP reactors details the characteristics of the melt's interaction with the sacrificial material (SM) and the patterns of subsequent cooling to crystallization temperature provided in the design of the trap.

From a physical standpoint, the selected model stages are justified by the phase transitions of the aggregate state of the system components including melting of the sacrificial material based on iron and aluminum oxides in the high-temperature corium melt during the initial period of their interaction and subsequent crystallization of the products of this interaction during intense external cooling of the trap body. Mathematical modeling is based on a generalized statement of the Stefan problem with free interfaces taking into account the residual radioactive heat release from the corium, the thermal effects of melting of iron oxides and redox reactions of oxides during oxidation of underoxidized elements in the melt, heat transfer by natural convection in the melt, heat transfer to cooling water through the shell walls and thermal radiation in the inner space.

The phenomenon of rapid gravitational inversion of immiscible oxide and metal components of different densities with molten oxides moving to the upper part of the melt pool and molten metals to the lower part is a natural delimitation of the model stages. Such a change in the pool structure appears due to a significant decrease in the density of the initially heavier oxide components of the melt

as compared to the metal ones after chemical interaction of the melt with the SM.

The COMSOL Multiphysics software package used in the computations does not create difficulties in solving the considered problems by end-to-end computation and analysis of thermokinetic processes in crucible-type ex-vessel melt retention devices, used in known specialized software codes developed for simulating various severe accident scenarios and their individual stages at the in-reactor stage.

The results obtained indicate that the thermokinetic processes considered generally provide a decrease in the temperature and density of the corium, a decrease in heat fluxes to the trap body, and a minimization of hydrogen and radioactive fission products. At the same time, the scatter in the estimates for the modes and times of cooling of the corium melt with uncertain composition requires in-depth consideration of the thermokinetics of crystallization processes, extremely important because of the risk of secondary centers with increased radioactivity appearing during local accumulation of heavier (relative to the entire melt) radioactive substance, as well as release of components into the gas phase. Their study at the next stages of the project can consist in refining the specifics of spatial kinetics of the computational model in the 3D statement, verifying and validating the model's applicability, in particular taking into account the problems of assessing the thermal state and the thermal stresses in the trap body.

This work was supported by a grant from the Russian Foundation for Basic Research (Project No. 19-08-01181).

REFERENCES

1. Walker S.J., Three-mile island: A nuclear crisis in historical perspective, University of California Press, Berkeley, 2004.
2. Abagyan A.A., Arshavskii I.M., Dmitriev V.M., et al., Computational analysis of the initial stage of the accident at the Chernobyl' atomic power plant, Atomic Energy. 71 (4) (1991) 785–795.
3. Gonzalez A.J., Akashi M., Boice J.D., et al., Radiological protection issues arising during and after the Fukushima nuclear reactor accident, Journal of Radiological Protection. 33 (3) (2013) 497–571.
4. Theofanous T.G., Lin C., Addition S., et al., In-vessel coolability and retention of a core melt, Nuclear Engineering and Design. 169 (1–3) (1997) 1–48.
5. Kim H.Y., Bechta S., Foit J., Hong S.W., In-vessel and ex-vessel corium stabilization in light water reactor, Science and Technology of Nuclear Installations. 2018 (2018) ID 3918150 (3 p).
6. Fischer M., Main features of the EPR melt retention concept (Rep. FZKA-6475), Forschungszentrum Karlsruhe GmbH Technik und Umwelt (Germany). 32 (14) (2000) 508–517; Proceedings of the OECD Workshop on Ex-Vessel Debris Coolability, Alsmeyer H. (Ed.), Karlsruhe, Germany, 15–18 November, 1999.
7. Bezlepkin V.V., Sidorov V.G., Kukhtevich V.O., et al., Ustroystvo lokalizatsii i okhlazhdeniya koriuma yadernogo reaktora [An arrangement to localize and cool down the nuclear reactor's



corium], Pat. No. 2514419, Russian Federation, MPK G21C 9/016.; SPb., OAO «Golovnoy Institut «VNIPIET» is a declarant and a patentee, No. 2012124161; declar. 20.02.14; publ. 27.04.2014, Bull. No. 23 (II Ch.). 11 p.

8. **Stolyarevskiy A.Ya.**, Spasayet li lovushka? [Does a trap rescue?], *Atomnaya Strategiya*. (4(89)) (2014) 16–18 (in Russian).

9. **Gusarov V.V., Almjashev V.I., Khabenskiy V.B., et al.**, Physicochemical modeling and analysis of the interaction between a core melt of the nuclear reactor and a sacrificial material, *Glass Physics and Chemistry*. 31 (1) (2005) 53–66.

10. **Asmolv V.G., Sulatskii A.A., Beshta S.V., et al.**, The interaction of nuclear reactor core melt with oxide sacrificial material of localization device for a nuclear power plant with water-moderated water-cooled power reactor, *High Temperature*. 2007. T. 45(1) (2007) 22–31.

11. Integral codes development and application for NPP safety analysis, *Proceedings of IBRAE RAS*, Ed. by L. A. Bolshov; Nuclear Safety Institute (IBRAE) RAS, Nauka, Moscow, 2011, Iss. 12 (in Russian).

12. **Lityshev A.V., Pantyushin S.I., Aulova O.V., et al.**, Experience in carrying out calculations of severe beyond design basis accidents for VVER RP using code SOKRAT, *Proceedings of the 9th International Scientific and Technical Conference “Safety Assurance of NPP with VVER”*, Podolsk, Russia, May 19–22, SCB “Gidropress”, Podolsk (2015) 1–22.

13. **Zvonarev Yu.A., Melnikov I.A., Shmelkov Yu.B.**, Simulation of corium pool behavior on RPV bottom under severe accident for VVER-1000, *Proceedings of the 10th International Scientific and Technical Conference “Safety Assurance of NPP with VVER”*, Podolsk, Russia, May 16–19, SCB “Gidropress”, Podolsk (2017) 1–22.

14. **Fiskov A.A., Bezlepkov V.V., Semashko S.Ye., et al.**, Opyt obosnovaniya ustroystva lokalizatsii rasplava LAES-2 [An experience on foundation for the arrangement of the melt localization at Leningrad NPP-2], *Proceedings of the Industry Research-to-Practice Conference «The Youth NFC: Science, Production, Ecological Safety»*, St. Petersburg, «Atomenergoprojekt», 2010. P. 5.

15. **Vasilenko V.A., Migrov Yu.A., Dragunov Yu.G., Bykov M.A.**, Heat-hydraulic design code KORSAR: Development status and experience, *Proceedings of the 3rd International Scientific and Technical Conference “Safety Assurance of NPP with VVER”*, Podolsk, Russia, May 26–30 2003, SCB “Gidropress”, Podolsk. 5 (3) (2003) 204–212.

16. **Sangiorgi M., Grah A., Pascal G., et al.**, In-vessel melt retention (IVMR) analysis of a VVER1000- NPP // JRC Technical Reports EUR 27951. JRC Science Hub, European Union, 2016. 250 p.

17. **Udalov Yu.P., Fedorov N.F., Soloveychik Ya., Pavlova E.A.**, Novyye funktsionalnyye oksidnyye materialy dlya yadernogo reaktorostroyeniya [New functional materials for nuclear rocket production], *Industry & Chemistry*. 80 (12) (2003) 3–10 (in Russian).

18. **Gusarov V.V., Almyashev V.I., Khabenskiy V.B., et al.**, Novyy klass funktsionalnykh materialov dlya ustroystva lokalizatsii rasplava aktivnoy zony yadernogo reaktora [A new class of functional materials for making the arrangement for localization the melt’s core region], *Rossiyskiy Khimicheskiy Zhurnal*. XLIX (4) (2005) 42–53 (in Russian).

19. **Stivens J.**, Posleavariynnyy otvod tepla ot oblomkov razrushennoy aktivnoy zony [Post-accident heat removal from the wreckage of the destroyed core], *Atomnaya Tekhnika za Rubezhom* (12) (1984) 14–22 (in Russian).

20. **Gusarov V.V., Almjashev V.I., Khabenskiy V.B., et al.**, Physicochemical simulation of the combustion of materials with the total endothermal effect, *Glass Physics and Chemistry*. 33 (5) (2007) 492–497.

21. **Lopukh D.B., Loginov I.A., Granovskii V.S., et al.**, Experimental investigation of processes arising when flooding a steel melt, *Thermal Engineering*. 48 (9) (2001) 725–731.

22. **Lagunenkov O.S., Krasnov V.O., Dovydkov S.A.**, Fuel in room 305/2. Probable formation scenario for nuclear-dangerous zones, *Problemi bezpeki atomnikh yelektrostantsiy i Chornobilya* [Safety Problems of Nuclear Power Plants and Chernobyl]. (24) (2015) 51–59 (in Russian).

23. **Almyashev V.I., Granovskiy V.S., Khabenskiy V.B., et al.**, Experimental study of corium melt oxidation processes in the reactor vessel, “*Tekhnologii Obespecheniya Zhiznennogo Tsikla Yadernykh Energeticheskikh Ustanovok*” [Maintenance Technology of the Life Cycle of Nuclear Power Installations]. (4 (10)) (2017) 59–84 (in Russian).

24. **Samarskiy A.A., Vabishchevich P.N.**, Vychislitel'naya teploperedacha [Computational heat transfer], Editorial URSS, Moscow, 2003 (in Russian).

25. **Snegiryov A.Yu.**, Chislennoye modelirovaniye turbulentykh techeniy [Numerical simulation of turbulent flows], Polytechnical Institute Publishing, St. Petersburg, 2009.

26. **Kutateladze S.S., Leontiev A.I.**, Heat transfer, mass transfer, and friction in turbulent boundary layers, Hemisphere, New York, 1990.

27. COMSOL Multiphysics, Software products COMSOL, Burlington, MA. URL: <https://www.comsol.ru>.

28. **Golovacheva V.G., Kovalenko A.N., Meshcheryakov D.K., et al.**, Correlation between heat – mass transfer, chemical reactions and phase transformations in corium melt localization devices during severe nuclear power plant accidents, Diversity in Nuclear: International

Youth Nuclear Congress (NIYNC2020), 8 –13 March 2020, Sydney, Australia (2020) 176–179.

29. **Voskov A.L., Dzuban A.V., Maksimov A.V.**, TernAPI program for ternary phase diagrams with isolated miscibility gaps calculation by the convex hull method, Fluid Phase Equilibria. 2015. Vol. 388 (25 February) (2015) 50–58.

30. **Konakov P.K., Vervovochkin G.E., Gorenkov L.A., et al.**, Teplo- i massoobmen pri poluchenii monokristallov [Heat and mass exchange when manufacturing monocrystals], Metallurgy Publishing, Moscow, 1971 (in Russian).

Received 20.07.2020, accepted 27.08.2020.

THE AUTHORS

KOVALENKO Anatoliy N.

Ioffe Physical Technical Institute of the Russian Academy of Sciences,

Peter the Great St. Petersburg Polytechnic University

26 Polytekhnicheskaya St., St. Petersburg, 194021, Russian Federation

ras-kan@mail.ru

KOPTYUKHOV Artem O.

NRC «Kurchatov Institute» – PNPI

Mc. Orlova Roshcha, Gatchina 1, Leningradskaya oblast, 188300, Russian

Federation

t44h@yandex.ru

MESHCHERYAKOV Dmitry K

Peter the Great St. Petersburg Polytechnic University

29 Politechnicheskaya St., St. Petersburg, 195251, Russian Federation

fess_i@bk.ru

SCHUKLINOV Alexey P.

JSC “Atomproekt”;

Peter the Great St. Petersburg Polytechnic University

82A Savushkina St., St. Petersburg, 197183, Russian Federation

mupol@mail.ru